JOURNAL OF BIOMEDICAL OPTICS 3(1), 85–95 (JANUARY 1998)

FUNDAMENTAL STUDIES OF FIBER-GUIDED SOFT TISSUE CUTTING BY MEANS OF PULSED MIDINFRARED LASERS AND THEIR APPLICATION IN URETEROTOMY

Ralf Brinkmann,[†] Ansgar Knipper,[‡] Gerit Dröge,[†] Frank Schröer,[†] Bernd Gromoll,[*] and Reginald Birngruber[†]

[†]Medical Laser Center Lübeck GmbH, Peter-Monnik-Weg 4, D-23562 Lübeck, Germany; [‡]Medical University Lübeck, Clinic of Urology, D-23562 Lübeck, Germany; [*]Medical University Lübeck, Institute of Pathology, D-23562 Lübeck, Germany

(Paper JBO-127 received Jan. 20, 1997; revised manuscript received July 21, 1997; accepted for publication Sep. 19, 1997.)

ABSTRACT

Fiber-guided ablation of soft tissue with pulsed holmium and thulium lasers was investigated for intraluminal incisions. A bare fiber/tissue-contact application system with a nearly tangential irradiation geometry was first used *in vitro* on porcine ureter tissue. The efficiency and precision of the method was analyzed for different laser and application parameters. The ablation dynamics in water and tissue was investigated by fast flash photography. Uniform cuts could be achieved with 200- and 318-μm fibers using a free-running holmium laser with a pulse repetition rate of 10 Hz and an average power of up to 4 W. The depth of the cuts could be increased by using a thulium laser with the same laser parameters. By reducing the pulse duration by one order of magnitude, the quality of the incisions was made more irregular, the zone of thermomechanical damage increased, and the cuts became deeper owing to the growing influence of cavitation on shorter laser pulse durations. In a first clinical trial, 20 patients underwent holmium laser therapy to reopen ureteral strictures. Neither bleeding nor other adverse effects due to the laser treatment occurred, showing IR laser ureterotomy to be a suitable and promising minimally invasive technique. © *1998 Society of Photo-Optical Instrumentation Engineers.* [S1083-3668(98)00401-8]

Keywords ablation; cavitation bubble; dynamics; holmium laser; incision; thermal damage; thulium laser; stenosis; ureteral stricture.

1 INTRODUCTION

Efficient and precise cutting of tissue by laser radiation requires sufficient energy to heat and evaporate the target and a wavelength exhibiting a strong absorption. An excellent chromophore in the mid-IR spectral range is water, which is present in high concentrations in most kinds of tissue. An efficient laser system in this regime is the CO_2 laser emitting at wavelengths around 10 μm and penetrating about 10 μm in water. While the CO_2 laser has proved its capability in medicine, its radiation cannot be transmitted by waveguides and can therefore only be applied superficially. Intracorporeal, minimally invasive applications require efficient fiber transmission of the laser energy, which is possible up to wavelengths of about 2.5 μm, thus including the water absorption peak at 1.94 μm. Efficient laser systems in this regime are holmium and thulium lasers emitting at wavelengths of 2.12 and 2.01 μm, respectively. The aim of this study was the evaluation of suitable laser irradiation parameters in the 2-μm spectral range to make controlled incisions in soft tissue, especially for intraluminal, minimally invasive surgery.

1.1 TISSUE ABLATION IN THE 2-μm SPECTRAL RANGE

The cutting of soft tissue (human skin, aorta, intestinal tissue) with laser radiation in the 2-μm spectrum was first investigated by Lane and Puliafito[1] using a cw Ho:YLF laser. They reported the quality of the incisions achieved to be comparable to that of CO_2 lasers. Most later tissue ablation studies have been performed with flashlamp-pumped holmium lasers irradiating the target perpendicularly either in a fiber contact or noncontact fashion. Ablation rates on hard (bone)[2] and soft tissue (rabbit liver, stomach, and colon)[3] have been measured *in vitro*. Oz et al.[4] ablated thrombogenic plaques on rabbits *in vivo* and found improved healing responses compared with those achieved with CO_2 lasers. Treat

Address all correspondence to Ralf Brinkmann. Tel.: 49 451 500 6500; Fax: 49 451 505 486; E-mail: brinkmann@mll.mu-luebeck.de

1083-3668/98/$10.00 © 1998 SPIE

et al.[5] used a holmium laser *in vivo* in a noncontact application in gastric tissue for laparotomy and gastrotomy. They found the tissue removal to be safe for underlying tissue (bowel wall at colon) and concluded that endoscopic surgery should benefit from this procedure. Nishioka and Domankevitz[6] compared holmium and thulium lasers with respect to ablation of rabbit liver *in vitro* and found comparable ablation rates, but a slightly lower threshold, and smaller thermally injured zones for the thulium laser.

Whenever short, strongly absorbed laser pulses are applied under liquid, it has to be kept in mind that vapor bubbles that expand with a high velocity are inevitably associated with the process. Different techniques to observe and analyze the ablation cavities in the mid-IR during the ablation of tissue *in vitro*[7] as well as *in vivo*[8] are described. Depending on the special absorption coefficient and pulse duration, high-pressure transients can occur at the onset of ablation and/or at the collapse of these cavitation bubbles. Pressure transients at the collapse of a holmium laser-generated bubble have been detected up to 200 bar normalized to 3 mm from the fiber tip[9] and 1.6 kbar at a 2-mm distance.[10] These pressure transients mainly depend on the size and form of the bubble, which is influenced by the diameter of the application fiber and the pulse energy and duration.[10,11] The influence of the cavitation bubble on irradiated soft tissue was first observed in laser angioplasty where a transient elevation of the intimal wall of the arteries was photographed while the laser radiation was applied in direct fiber/tissue contact.[12] It therefore can be expected that cavitation dynamics will significantly influence the ablation process.

1.2 URETERAL STRICTURES

Obstructive uropathy owing to ureteral strictures are often a consequence of infections in the urinary tract following open surgery, endourological manipulation, or nonoperative inflammations, which are the most frequent with extrinsic compression and radiation therapy. Congenital stenoses are seen at the ureteropelvic junction, with ureteral valves, or with an obstructed megaureter. Untreated strictures lead to a dilation of the upper urinary tract, which is often followed by the destruction of the renal parenchyme with impairment of renal function. This may finally lead to total loss of the kidney via chronic urinary congestion.

Different surgical procedures have been developed to resolve these strictures, according to location and etiology. The bladder hitch procedure is applied in the case of distal strictures; ureteropyeloplasty is used for ureteropelvic junction stenoses; whereas lesions in the midureter require autotransplantation of the kidney into the inguinal fossa or intestinal interposition. Endoscopic techniques have also been introduced. They include ureteral stenting (double J stent), balloon dilation, and ureterotomy with a small cold knife or high-density current, based on the idea of intubated ureterotomy.[13] The success rates of these minimally invasive techniques range between 50 and 90% in the literature, with high stricture recurrence rates.[14,15] The reasons proposed for these complications are large scars and high traumatic effects due to the techniques and the instruments required for them.

1.3 LASER URETEROTOMY

Lasers have been used to make incisions in the urinary tract. Transurethral incisions to open strictures or small obstructive prostates have been done, for example, by Malek using a frequency-doubled Nd:YAG laser at a wavelength of 532 nm.[16] However, owing to the low absorption of light in the visible and near IR spectrum, the use of high average laser power in this spectral range is indispensable, resulting in a large thermal necrosis zone. Johnson, Cromeens, and Price[17] conducted noncontact dosimetry studies on ureteral tissue *in vitro* with a holmium laser.

The anticipated advantages of laser systems able to perform small and well-defined ureteral incisions are the minimal traumatic and adverse effects on the tissue to be incised. A small and flexible fiber in combination with a semirigid small endoscope or even a steerable catheter can be used, with a subsequent reduction of invasiveness and morbidity. These treatments also reduce hospitalization time, since the routine treatment of ureteral strictures is either open surgery or endoscopic techniques requiring thick and rigid instrumentation.

Laser ureterotomy requires a longitudinal cut over the typical stenosis length of several centimeters through the ureteral mucosa up to the periureteral fat.[18] Ideally, the required complete ureteral wall dissection of approximately 1 mm in depth should be performed by making only one pass over the tissue. The application has to be safe, strictly excluding any risk of perforation, even if the laser is fired for several seconds on the same location.

To evaluate the appropriate laser and application parameters, we performed an *in vitro* study on enucleated, opened pig ureters by using two laser systems to qualitatively and quantitatively analyze the laser incisions. Holmium laser (Cr:Tm:Ho:YAG, $\lambda = 2.1\ \mu$m) radiation is strongly absorbed by water having an absorption coefficient of $\mu_a = 23.8\ \text{cm}^{-1}$,[19] with a penetration depth ($1/e$ attenuation) of 420 μm. Thulium laser radiation (Cr:Tm:YAG, $\lambda = 2.01\ \mu$m) is even more strongly absorbed ($\mu_a = 61.9\ \text{cm}^{-1}$),[19] with a penetration depth of only 162 μm.

Since the ablation of tissue should be effective *and* safe, one has to pay attention to the ablation dynamics during laser exposure, and thermomechanical damage ranges have to be investigated. There-

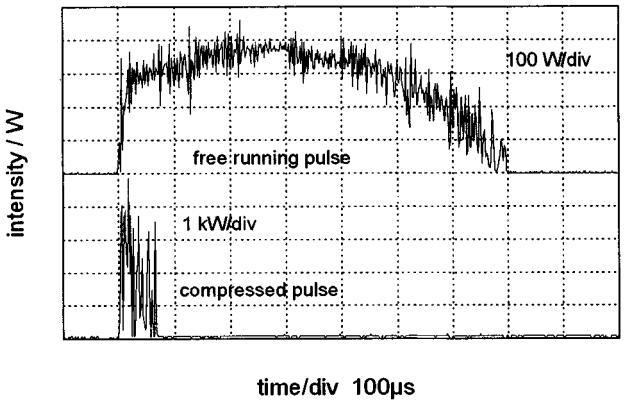

Fig. 1 Pulse shapes of 200-mJ holmium laser pulses, in the free-running and pulse-compressed mode with pulse lengths of 600 and 60 μs FWHM, respectively.

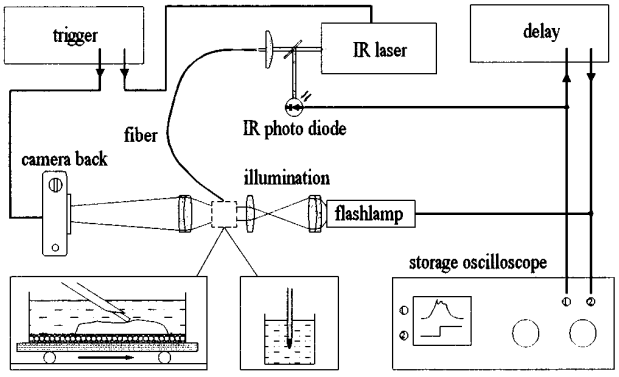

Fig. 2 Experimental setup to investigate ablation dynamics in water or on tissue by fast flash photography.

fore we used fast flash photography to analyze the dynamics of ablation and the influence of cavitation effects on the shape of the incision. Furthermore, we performed histomorphometry to quantitatively determine the thermomechanical damage range.

2 MATERIALS AND METHODS

2.1 LASER AND APPLICATION SYSTEM

The laser system used was a unit developed by us and equipped with a linear laser cavity that could be used with either a holmium or a thulium laser rod as active medium. The system could be operated with a pulse repetition rate up to 20 Hz. Single-pulse energies of 2 J were generated, while at a frequency of 10 Hz, 1 J was achieved, giving an average power of 10 W. In a free-running mode, the pulse duration depends on the duration of the electric discharge driving the flashlamp, and the cavity configuration. Typically, the pulse length of a 200-mJ pulse was 600 μs full-width at half-maximum (FWHM), and 700 μs over all (Figure 1).

To generate shorter pulse lengths, the rear, high-reflecting mirror of the cavity was replaced by a rotating mirror. In this case the pulse length mainly depends on the rotating speed of the mirror determining the opening time of the laser cavity and the Q-factor of the resonator.[20] To achieve pulse durations on the order of 60 μs FWHM, the rotational speed needed was 1500 rpm. Compared with the free-running operation, the pulse energies were typically reduced by a factor of 2. The rotating mirror technique was used for all incisional experiments. To improve the pulse-to-pulse stability which was necessary to record the cavitation dynamics, the rotating mirror was replaced by a rotating disk having a 5-mm diameter bore at a distance of 39 mm from its axis. To achieve the same pulse length of 60 μs, the rotating speed had to be 15,000 rpm. A typical pulse shape is shown in Figure 1. Both methods allowed us to generate any pulse duration between several hundred nanoseconds and the free-running pulse length. In this study we operated the laser in the free-running and the so-called pulse-compressed mode with typical pulse lengths of around 600 and 60 μs, respectively. Low-OH all-silica fibers (Ceram Optec, Optran WF, acrylat coated) of 200/220- and 318/350-μm (core/cladding) diameter were used.

2.2 EXPERIMENTAL SETUP AND *IN VITRO* STUDY

The experimental setup to make the laser incisions and measurements of the cavitation bubble dynamics is shown in Figure 2. The laser system and the camera (Olympus, OM2) were triggered by an external pulse generator. The laser system was always operated at a pulse repetition rate of 10 Hz, except that single pulses were used for fast flash photography.

To record ablation dynamics, the event was illuminated by a flashlamp pulse, 150 ns in duration (high-speed photosystem, FX-xenon flashlamp). To minimize jitter problems, the flashlamp was directly triggered by the first spike of the laser pulse, which was detected with a fast IR photodiode (EG&G Judson, J12-5AP-R02M). The delay time from trigger to flash was 3 μs. To photograph at any time within the ablation process, a variable delay relative to the onset of the laser pulse was integrated (Stanford Research Systems, Inc., model DG 535) and monitored on a storage oscilloscope (Tektronix, TDS 540). However, this means that a series in the ablation cycle as shown here does not represent a single event; each picture corresponds to a different laser pulse.

The object was illuminated by a Köhler setup (condensor, Pentacon, 50 mm f/1.8; collimator, achromat 50 mm) providing a collimated beam 5 mm in diameter. Photographs were taken with a 63-mm objective (Nikon, el-Nikkor 63-mm f/2.8N) and a standard film (Agfa CTi 100). A magnification of 7:1 was achieved with a space of 460 mm between camera back and objective. The quartz cuvette contained either pure water to record the cavitation

bubble dynamics in this medium or ureter tissue to be incised. Therefore, freshly harvested porcine ureters were used. The ureter tissue was mounted on an x-step motor drive and immersed in a 0.9% saline solution. The fiber was guided by a canula fixed at an angle of 10 deg to the tissue. The last 10 mm of the fiber tip were unguided in order to use the flexibility of the fiber to compensate for tissue surface irregularities and to guarantee tissue contact. During the cutting procedure, the x-step was always moved with a constant velocity of $v = 0.25$ mm/s against the fixed fiber.

Every set of irradiation parameters was obtained on three different specimens with a cutting length of several centimeters. All ureteral cuts were documented by photography and then fixed in 5% formalin. Three different sections of every cut were chosen for histomorphometry. The shape of the incisions and the damage zones were determined with a computerized morphometry system (Zeiss-Kontron Videoplan) after paraffin embedding and hematoxylin-eosin staining (HE).[18] Enhanced coloration with HE showed the areas of thermal damage, dissections within the tissue, and the mechanical damage range.

2.3 CLINICAL STUDY

For the clinical study, we operated the holmium laser at a 10-Hz pulse repetition rate in the free-running pulse mode with a pulse energy of 300 mJ (average power of 3 W) and used a 318-μm core diameter fiber. A 7.5 F semirigid ureteroscope (Wolf) with a working channel diameter of 3 F was chosen. The laser fiber was introduced into a standard ureter catheter (Rösch, 3F) to protect the fiber, especially the distal fiber tip, from any mechanical damage during the passage through the working channel of the endoscope. Twenty patients (16 female, 4 male, aged 15 to 83 years, av. 52 years) were treated with 7 primary and 13 secondary strictures having a length between 0.5 and 3 cm. The strictures were located in the lower ureter tract (7), the ureteropelvic junction (12), and at the ureterointestinal anastomosis (1). After the operation, a 9 F double J ureteral stent with a 12 F movable sheath was inserted into the upper urinary tract.

3 RESULTS

3.1 INCISION PARAMETERS *IN VITRO*

Figure 3 shows the incision data as a function of average power for a holmium laser operated in the free-running mode with a 318-μm fiber. Incision width and depth as well as the thermomechanically altered zone were found to increase with increasing laser power while the coagulation depth remained almost constant around 350 μm. At an average laser power of 4 W, an onset of tissue carbonization was observed and denatured tissue partly began to stick at the fiber tip, reducing both the incision depth

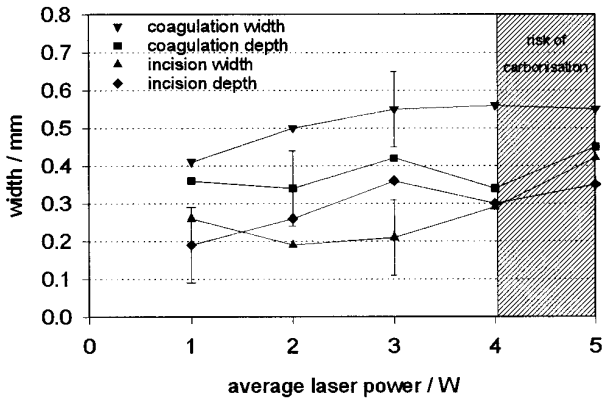

Fig. 3 Incision data achieved *in vitro* with a free-running holmium laser on porcine ureter tissue. Fiber core diameter, 318 μm; prf, 10 Hz; cutting speed, 0.25 mm/s.

and the quality of the cuts. A less uniform incision was also achieved by using cutting speeds of 0.5 mm/s and higher.

Figure 4 shows the incision depth, the most significant parameter for laser ureterotomy, versus average laser power for the holmium and thulium laser in comparison to the free-running and the pulse compressed mode, respectively. Regarding the holmium laser, the incision depth for the same laser power is increased up to a factor of 4 (at 3 W) by applying shorter pulses. The width of the incision channel is 50% larger than the fiber diameter in the free-running pulse application with a uniform profile (Figure 5), whereas the channel is extremely enlarged and shows a significantly reduced cutting quality in the pulse-compressed mode, as shown in Figure 7. The corresponding histology (Figure 8) shows, beneath the thermally damaged zone, huge mechanical dissections, which are significantly less marked in the case of the free-running pulse mode (Figure 6). The lateral thermomechanical damage

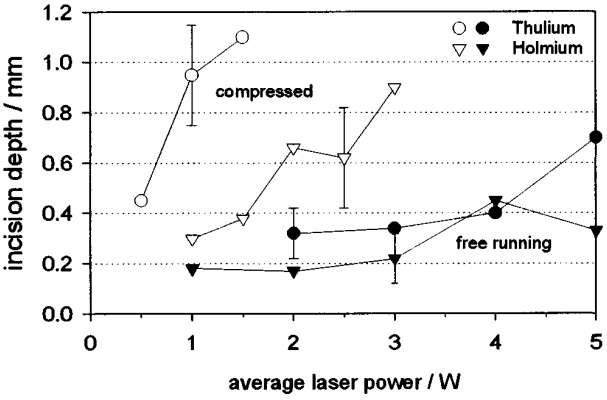

Fig. 4 Incision depth achieved *in vitro* with a holmium and thulium laser in the free-running and pulse-compressed mode on porcine ureter tissue. Fiber core diameter, 200 μm; prf, 10 Hz; cutting speed, 0.25 mm/s.

Fig. 5 Microscopic photograph of an *in vitro* holmium laser incision achieved in the free-running mode. Fiber, 200 μm; average laser power, 2 W; prf, 10 Hz; cutting speed, 0.25 mm/s. The histology shown represents the upper limit of channel dimensions with these parameters.

Fig. 7 Microscopic photograph of an *in vitro* holmium laser incision achieved in the pulse-compressed mode. Fiber, 200 μm; average laser power, 2 W; prf, 10 Hz; cutting speed, 0.25 mm/s. The incision is very irregular. The incision width varies between 300 and 800 μm.

zone, defined by coagulation and dissections, was found to be about twice as large in the pulse-compressed mode.

Furthermore, Figure 4 demonstrates that application of the stronger absorbed thulium laser radiation led to an increase in incision depth for both pulse modalities compared with that of the holmium laser. Working with only 1.5 W average power in the pulse-compressed mode, the clinically desired cutting depth of approximately 1 mm could be achieved.

3.2 CAVITATION BUBBLE DYNAMICS IN WATER

Fast flash photography, as illustrated in Figure 9, demonstrated the different cavitation bubble dynamics of both pulse modalities by applying holmium laser pulses of 200 mJ through a 318-μm fiber in water. Figure 9(a) shows a growing cavitation bubble at the fiber tip 50 μs after the onset of a 600 μs laser pulse. Between 50 and 150 μs, the bubble expands with an average axial speed of about 7 m/s, reaching its maximal lateral extent after 250 μs. Heating and evaporation of water takes place at the distal end of the bubble, leading to an aspherical cavity. During the collapse phase of the first part of the bubble, the distal part is still expanding. In the collapse, which takes place after about 500 μs, part of the kinetic bubble energy is converted to heat. The water, which is heated by the direct laser exposure and by the bubble collapse, becomes visible in the form of thermal refractive index fluctuations (thermal schlieren) where cold surrounding water is mixed with heated water, which is clearly observed beneath the fiber tip. The maximal dimension of the bubble is reached after 550 μs, with a lateral diameter of 1.75 mm and a distance to the fiber tip of 2.5 mm. After 800 μs, the distal part of the cavitation bubble collapses.

Figure 9(b) shows the dynamics after a 60-μs laser pulse. Within the first 100 μs, the bubble expands with an average speed of 14 m/s. An almost spherical bubble reaches its maximal diameter of about 2.8 mm 150 μs after the onset of the pulse and collapses further on. During the collapse phase, radial thermal schlieren at the outer rim of the bubble are observed (pictures taken at 300 and 310 μs). At 320 μs, the collapse has already occurred and the thermal schlieren lean tangentially on the regrowing bubble in the postcollapse phase. Owing to the slightly irregular collapse, disturbed by the

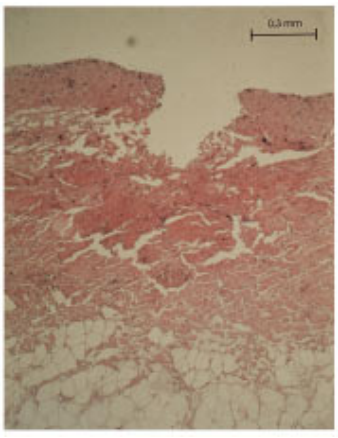

Fig. 6 Hematoxylin-eosin-stained histology corresponding to Figure 5, showing an incision width of 350 μm and a depth of 400 μm. The coagulation width is about 500 μm.

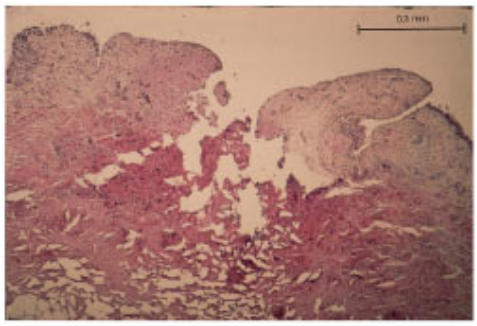

Fig. 8 Hematoxylin-eosin-stained histology corresponding to Figure 7. The thermomechanical damage zone varies between 200 and 500 μm; the incision channel is filled with debris.

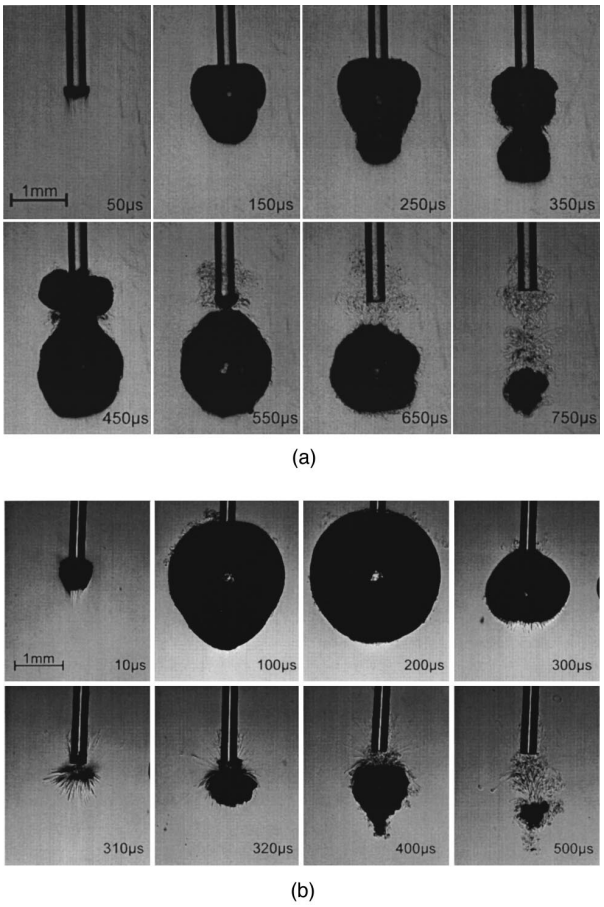

Fig. 9 Cavitation bubble dynamics in water. The time of photography after onset of the holmium laser pulse is indicated. Energy, 200 mJ; fiber, 318 μm. (a) Free-running mode, pulse duration, 600 μs. The onset of ablation is observed about 50 μs after the pulse begins; a first collapse takes place after 550 μs. Schlieren are observed after the collapse. (b) Pulse-compressed mode, pulse duration, 60 μs. The onset of ablation is observed a few microseconds after the pulse begins; the bubble shape becomes spherical and collapses after 310 μs. Schlieren are observed during and after bubble collapse phase.

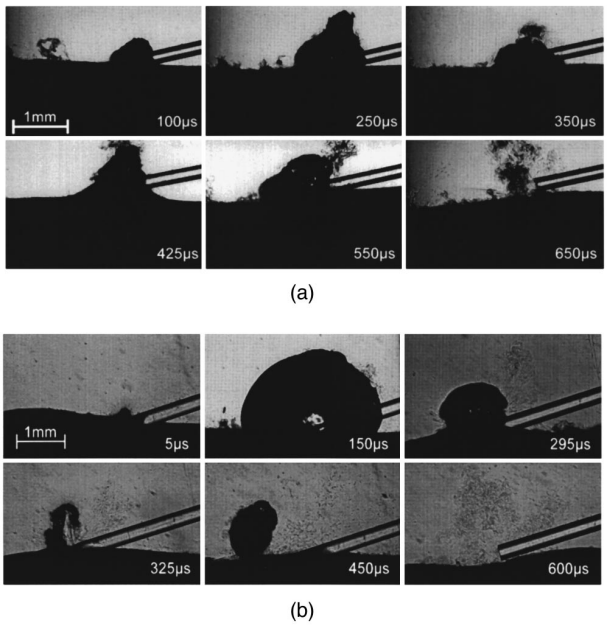

Fig. 10 Ureter tissue ablation in water. The time after onset of the holmium laser pulse is indicated. Energy, 200 mJ; fiber, 318 μm. (a) Free-running mode, pulse duration, 600 μs. (b) Pulse-compressed mode, pulse duration, 60 μs.

fiber, the bubble regrowth is aspherical. A second collapse is observed after about 500 μs.

3.3 ABLATION DYNAMICS ON TISSUE

By applying free-running laser pulses to tissue, ablation, as is obvious in Figure 10(a) by the irregular dark areas, is observed during nearly the whole time of exposure. Tissue elevation (which is especially seen in the series shown after 425 μs by the smooth rim on the left) was observed in some cases. With a 60-μs pulse [Figure 10(b)], a semispherical bubble with a maximal radius of 1.8 mm was recorded after about 150 μs, with a subsequent collapse after about 300 μs. The collapse time was nearly the same as in water. Ablation products were not observed prior to the collapse.

Figure 11 shows photographs of the ablation site in top view and cross section after a single laser pulse was applied. In the free-running pulse mode, an ellipsoidal-shaped ablation site [Figure 11(a), cross section] with a comparable size of residual damage probably caused by the cavitation bubble [Figure 11(a), top view] was found. In the pulse-compressed mode [Figure 11(b)], the damage zone was found to be much larger and corresponded to the maximal size of the cavitation bubble observed at tissue ablation [Figure 10(b)]. In both cases, the maximal extension of the bubble could be observed by tissue displacement on the surface confirming the results of fast flash photography.

3.4 CLINICAL RESULTS

Between March 1994 and February 1995, 20 patients underwent holmium laser ureterotomy. The clinical procedure revealed an average operation time of 33 ± 9 min; the actual time for laser treatment took 18.1 ± 8.6 min. The total laser time was 4.6 ± 1.8 min, corresponding to an average of 2760 laser pulses applied with an overall energy of 828 J. Three to five cuts through the incision channel had to be performed to achieve a complete ureteral wall dissection. The average number of passes over the stenosis needed were 2.3 ± 1.2. The whole operation was observed and recorded by videoscopy. No bleeding could be seen and no complications due to the laser treatment occurred.

During the learning phase, the laser treatment time could be reduced from 26 ± 11 min (first 6 patients) to 16 ± 3 min (last 6 patients) and the average number of incisions applied from 3.5 ± 0.8 to 1.2 ± 0.4, while the average laser-on time (from 5.2

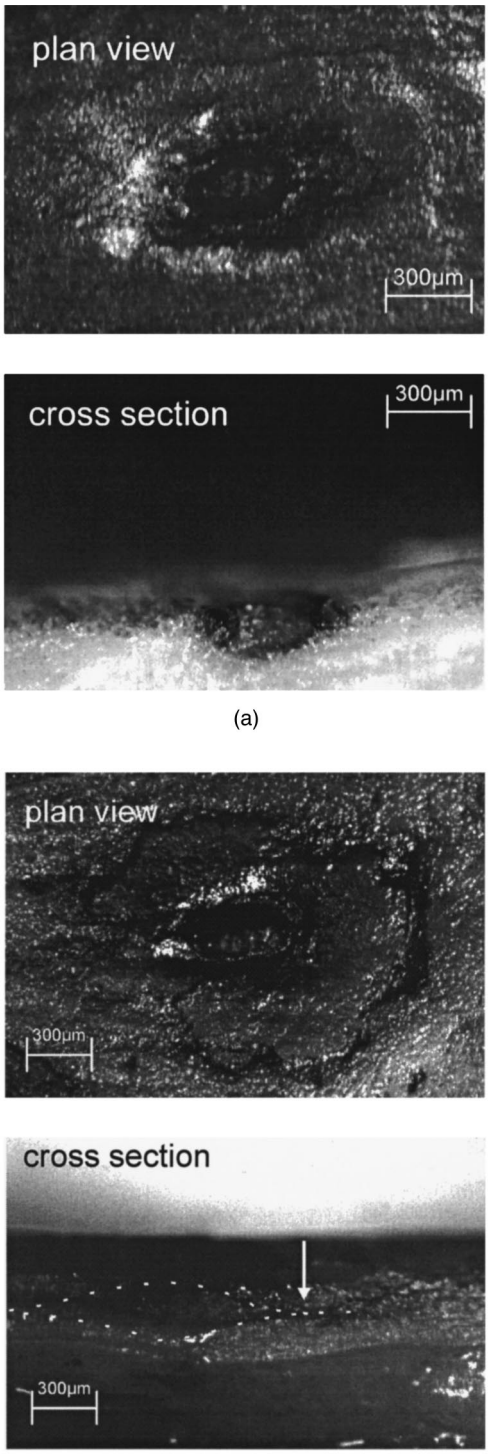

Fig. 11 Microscopic photographs of single laser ablation sites in plain view and cross section achieved with the holmium laser. The fiber was introduced from the left side and placed under an angle of 10 deg to the ureter tissue, the bare fiber tip in contact with the tissue. (a) free running mode, pulse duration, 600 μs. (b) Pulse-compressed mode, pulse duration 60 μs. The dashed line shows the ablation crater, the arrow indicates dye penetrated into the tissue pointing out dissections resulting from cavitation. The central crater shows the ablation side while the outer rim shows the maximal extension of the cavitation bubble demarked by tissue displacement.

± 1.5 min to 4.7 ± 2.3 min) remains nearly unchanged.

In the follow-up period of up to 15 months, the ureter function was controlled by intravenous pyelogram (IVP) and iodine-123 hippurane clearance. Treatment was considered successful when there was objective evidence of improvement in the anatomical configuration, that is, resolution of the stricture. As summarized in Table 1, the endoscopic approach was successful on 11 of the 20 patients (55%). Of the 9 failures, 3 underwent successful open repair for strictures longer than 1 cm. Two patients underwent nephrectomy in view of no improvement and poor renal function. All of these kidneys had impaired function demonstrated preoperatively on an IVP and renal scan. The last 4 failures were judged as static. These patients were asymptomatic, with a relatively large ureteral lumen without evidence of deterioration of renal function.

4 DISCUSSION

In order to investigate the intraluminal cutting of soft tissue, different laser and application parameters were investigated *in vitro*. We focused on direct fiber tissue contact, which provides the smallest possible application system and can generally be performed endoscopically in tubed hollow organs by the smallest and most flexible instrumentation. To explain the different ablation rates and incision qualities achieved in the free-running and pulse-compressed mode, we investigated the ablation dynamics by fast flash photography in water and on tissue.

4.1 CAVITATION BUBBLE DYNAMICS IN WATER

Cavitation bubbles observed by flash photography showed long aspherical bubbles when free-running holmium laser pulses were applied in water, while in the pulse-compressed mode, nearly spherical bubbles having a 60% larger lateral extent were seen. The difference in bubble size is due to the lifetime of the bubble in relation to the laser pulse duration[8] and to the pressure in the initial bubble volume at the fiber tip, which increases towards shorter pulse durations. If the bubble lifetime is much longer than the laser pulse duration, a nearly spherical bubble appears, and thus a spherical symmetric collapse can occur, emitting high-pressure waves. With a 200-mJ, 60-μs holmium laser pulse, a bubble lifetime of 310 μs until the first collapse was measured. This result is in close agreement with the data of Jansen et al.,[11] who measured bubble lifetimes of 300 μs by applying 200-mJ holmium laser pulses in water, although a 100-μs laser pulse duration was used and the pulses were applied by a 200-μm fiber. This shows that the formula of Rayleigh[21] relating the bubble lifetime to its radius can be applied if the bubble shape is spherical. Our

Table 1 Data of patients who underwent holmium laser ureterotomy . All laser treatments were initially successful, and the results indicate the clinical outcome at the end of the follow-up period.

No.	Age (years)	Sex	Cause	Location[a]	Side	Follow-up (months)	Result
1	59	Female	Secondary	Distal	Right	24	Successful
2	73	Female	Secondary	UPJ	Right	12	Unchanged
3	37	Female	Primary	Middle	Right	24	Successful
4	36	Female	Secondary	UPJ	Right	15	Successful
5	19	Male	Primary	UPJ	Right	15	Successful
6	49	Female	Secondary	Distal	Right	15	Successful
7	64	Female	Secondary	UIA	Left	18	Successful
8	61	Male	Primary	UPJ	Right	3	Unsuccessful
9	74	Female	Secondary	Distal	Right	12	Unchanged
10	84	Female	Secondary	Distal	Right	12	Unchanged
11	39	Female	Secondary	UPJ	Right	12	Successful
12	61	Female	Secondary	Distal	Right	15	Successful
13	16	Female	Secondary	UPJ	Left	3	Unsuccessful
14	67	Female	Secondary	UPJ	Right	6	Unsuccessful
15	53	Male	Primary	UPJ	Right	9	Successful
16	63	Female	Secondary	Distal	Left	6	Successful
17	17	Female	Secondary	UPJ	Right	6	Unchanged
19	28	Male	Primary	UPJ	Left	6	Unchanged
20	54	Female	Primary	UPJ	Right	9	Successful

[a] UPJ, uretopelvic junction; UIA, ureterointestinal anastomosis.

data for 60-μs pulse durations fit this theory, as did the data achieved with 100-μs and 500-ns pulses[11] and 40 ns.[10] We always found spherical bubble shapes for pulse durations below about 80 μs.

With much longer pulses in water, the bubble shape becomes highly aspherical and the transient geometry of the bubble strongly depends not only on the pulse duration but also on the pulse energy and the fiber diameter. We used a free-running holmium laser with a pulse duration of 600 μs. After bubble formation took place, the energy was transmitted through the growing cavitation bubble, leading to water evaporation at the front surface of the expanding bubble, which subsequently resulted in a long aspherical bubble. This so-called Moses effect[22] has been measured and described in the 2-μm wavelength range.[7] If parts of the bubble near the fiber tip collapse during the laser pulse, vapor channels and several partly separated bubbles may be observed.

4.2 SINGLE-PULSE TISSUE ABLATION DYNAMICS

With single laser pulses on tissue in the free-running mode, ablation took place over nearly the entire duration of pulse emission. An irregular steam bubble occurred that had approximately the same lifetime as in water and led to tissue elevation in front of the fiber. This tissue elevation is comparable to that observed in laser angioplasty, where a transient lift of the intimal wall of arteries was photographed at a perpendicular fiber contact.[12] The bubble did not extend far outside the ablation crater and only a shallow rim of denatured tissue could be observed, as shown in Figure 11(a).

In the pulse-compressed mode, a semispherical bubble with a radius of 1.8 mm, which is 28% larger than the radius of a spherical bubble in water, was observed on tissue. Calculations of the bubble volume yielded nearly the same value for both cases,

$V = 11.5\ mm^3$ and $V = 12.2\ mm^3$ in water and in tissue, respectively. Significant tissue ablation could not be observed prior to the collapse of the bubble [Figure 10(b)]. Tissue denaturation and displacement were found up to the maximal radius of the bubble on the surface, as shown in Figure 11(b). The axial and lateral extent as well as the depth of single pulse craters did not differ significantly in either pulse modality (Figure 11). However, for intraluminal application, one has to keep in mind that the bubble diameter may greatly extend the free lumen of the ureter. This subsequently leads to overstretching of the tissue owing to cavitation effects, as illustrated on a model for laser angioplasty.[23]

4.3 CUTTING OF SOFT TISSUE

The ablation of tissue in a comparison of both pulse modalities showed substantial differences. In the free-running mode, small and precise cuts in the dimension of the fiber used could be achieved, whereas in the pulse-compressed mode, much broader and deeper incision channels were produced, although their quality was more irregular. The reasons were revealed by flash photography.

Cavitation bubble dynamics seems to be responsible for the different cutting qualities found for both pulse durations. When free-running pulse trains were applied during the incision procedure, the bubbles extended into the already ablated channel without evident ablation at the channel rim. The smoothest cut was achieved in this way with the holmium laser. In the pulse-compressed mode, due to the explosive evaporation and huge extension of the bubble, pulse trains led to a significant and irregular broadening of the incision channel up to the maximal diameter of the semispherical cavitation bubble. In both pulse modalities, lateral tissue displacement plays a major role and becomes more dominant for shorter pulse durations.

The cavitation bubble dynamics seems also to be responsible for the relatively low cutting speed necessary for high-quality cuts. To achieve a uniform cut, a cutting speed of 0.25 mm/s at a pulse repetition rate of 10 Hz was needed, meaning the fiber has to be pulled for about 25 μm from pulse to pulse. On the other hand, the axial length of the ablation crater achieved with a single pulse is about 450 μm (Figure 11), which should allow about a tenfold higher cutting speed. Since the fiber is moved in the antegrade direction, it can be concluded that material was ejected or elevated into the previously ablated channel, and following pulses were needed to substantially evaporate this tissue. Increasing the cutting speed above 0.5 mm/s resulted in a nonuniform incision and an incomplete ureter wall dissection.

With regard to clinical applications, an important parameter is the incision depth. For laser ureterotomy, it is advantageous to achieve a cutting depth of about 1 mm, which is required for a complete ureteral wall dissection, with only one pass. Using the holmium laser in the free-running mode, the depth of the cuts increased linearly from 200 μm at 1 W to 350 μm at 4 W (deviation about 100 μm) with a uniform and homogeneous incision quality. The incision width was on the order of the fiber diameter and the coagulation zone corresponded to the penetration depth of the laser radiation, as expected. The useful power range was limited to approximately 4 W, independent of the fiber diameter.[24] At a higher average laser power, tissue was found to stick at the fiber tip and the onset of carbonization was observed.

If the holmium laser was run with the same average laser power in the pulse-compressed mode, the incision depth could be increased significantly, up to a factor of 4 at 3 W. The most likely reason is that the cavitation process supports the ablation, as discussed earlier.

A further increase of incision depth was achieved by working with the thulium laser. Although the penetration depth of this laser radiation in water (the main absorber in tissue at this wavelength) is 2.6 times less than that of the holmium laser, we found an increase in incision depth of approximately a factor of 2, which is on the order of that predicted by simple ablation models near threshold radiant exposure.[25,26] Since the ablation rate increases with increasing absorption, higher amounts of tissue will be ablated at the same radiant exposure with the thulium laser. This is in contrast to the results of Nishioka et al., who found only minimal differences in ablation rates comparing both laser systems.[6] However, they applied the laser radiation perpendicular to the tissue in an air–tissue interface. The difference with our result may also be attributed to the nearly tangential application as well as to the cavitation bubble due to the liquid environment. Because a larger absorption coefficient leads to an increased bubble diameter, the ''Moses effect'' enables the transmission of radiation into deeper zones of the irradiated target.

The lateral coagulation zone was decreased by using the thulium laser, as expected for a shorter penetration depth of radiation. Operating this laser in the pulse-compressed mode with an average power of 1 to 1.5 W, an incision depth of 1 mm can be achieved with only one pass, which is desirable in laser ureterotomy.

4.4 CLINICAL STUDY

During the past 2 years, intubated ureterotomy has evolved as the treatment of choice for primary and secondary obstructions of the ureter. In a first clinical study, 20 patients were treated with a free-running holmium laser. With this laser mode, the most uniform and precise cuts with the lowest thermomechanical damage were achieved *in vitro* and the best healing response could be expected. Laser ureterotomy provided an easily handleable incision

procedure and the technique was proved to be safe and suitable. This is demonstrated by the operation time of approximately only 18 min, where no complications due to the laser treatment occurred at any time, and working under clear vision was always guaranteed.

Primary and secondary obstructions of the ureter responded equally well during the long term, with the success rate in both groups of patients being 55%. Of these 20 patients, 12 have been followed for longer than 12 months. It became apparent that if a stenosis of the ureter does not repair within 6 months after removal of the ureteral stent, then a later failure is most unlikely. Most important, one must realize that avascular obstructions longer than 3 cm are not correctable with ureterotomy.

Our initial expectation that laser ureterotomy would provide increased long-term success rates compared with the conventional cold knife technique because of less trauma to the ureteral tissue could not be proven in the first trial. However, the main advantage of laser ureterotomy is its minimally invasive characteristics and the reduced morbidity of the patient. A second trial is planned with a pulse-compressed thulium laser. If the healing response is found to be comparable, thulium will be the laser of choice, because the required ureteral incision can be obtained by only one pass, which is a further and significant improvement of the method.

5 CONCLUSION

IR laser ablation in the 2-μm spectral range was proved to be a precise method for making well-defined incisions in soft tissue. Using flashlamp-pumped lasers, ablation rates and cutting quality may be influenced widely not only by the pulse energy and repetition rate but also by the wavelength, and especially by the pulse duration. Toward shorter pulse durations, the ablation becomes more explosive due to the more spherical size of the cavitation bubble, its increased diameter and speed of expansion, as well as a pronounced collapse.

A further influence on the ablation characteristics can be exerted by the choice of the application system and its irradiation characteristics. In laser ureterotomy, the fiber–tissue contact application, where the fiber tip is guided nearly tangentially in an antegrade direction over the length of the stenosis, provides maximum control and safety. The risk of ureteral perforation is extremely small since the energy is applied almost tangentially to the ureter wall.

The main advantage of laser ureterotomy over other techniques (gold standard: open surgery) is minimally invasive surgery by use of small flexible or semiflexible ureteroscopes. Further advantages are the easy and safe incision procedure, reduced adverse tissue effects, and the absence of bleeding, which guarantees clear vision during the operation. The laser treatment demonstrated a significant reduction in morbidity, and a reduced hospitalization time can be expected.

Besides laser ureterotomy, the method described here shows a high potential for comparable medical problems (e.g., ablation or dissections in the urethra or other small-tubed organs) for example, in gastroenterology or gynecology. For applications not requiring a precisely defined incision depth, the cutting speed can be improved by increasing the pulse repetition rate. The incision depth may be improved by a modified application system that irradiates the tissue more perpendicularly (side-fire techniques).

REFERENCES

1. R. J. Lane and C. A. Puliafito, ''Comparative study of the surgical application of the holmium and CO_2 laser,'' *Lasers Surg. Med.* **6**, 259 (1986).
2. R. C. Nuss, R. L. Fabian, R. Sarkar, and C. A. Puliafito, ''Infrared laser bone ablation,'' *Lasers Surg. Med.* **8**, 381–391 (1988).
3. N. S. Nishioka, Y. Domankevitz, T. J. Flotte, and R. R. Anderson, ''Ablation of rabbit liver, stomach and colon with a pulsed holmium laser,'' *Gastroenterology* **96**, 831–837 (1989).
4. M. C. Oz, M. R. Treat, S. L. Trokel, J. E. Andrew, and R. Nowygrod, ''A fiberoptic midinfrared laser with CO_2 laser-like effect: application to atherosclerosis,'' *J. Surg Res.* **47**, 493–501 (1989).
5. M. R. Treat, S. L. Trokel, V. J. DeFilippi, J. Andrew, and M. G. Cohen, ''Mid-infrared lasers for endoscopic surgery,'' *Am. Surgeon* **55**, 81–84 (1989).
6. N. S. Nishioka and Y. Domankevitz, ''Comparison of tissue ablation with pulsed holmium and thulium lasers,'' *IEEE J. Quant Elect.* **26**(12), 2271–2275 (1990).
7. T. G. van Leeuwen, M. J. van der Veen, R. M. Verdaasdonk, and C. Borst, ''Noncontact tissue ablation by holmium: YSGG laser pulses in blood,'' *Lasers Surg. Med.* **11**, 26–34 (1991).
8. R. Brinkmann, C. Hansen, D. Mohrenstecher, M. Scheu, and R. Birngruber, ''Analysis of cavitation dynamics during pulsed laser tissue ablation by optical on-line monitoring,'' *IEEE J. Selc. Top. Quant. Elect.* **2**(4), 826–835 (1996).
9. T. Asshauer, K. Rink, and G. Delacrétaz, ''Acoustic transient generation by holmium-laser-induced cavitation bubbles,'' *J. Appl. Phys.* **76**, 5007–5013 (1994).
10. M. Frenz, H. Pratisto, F. Könz, and E. D. Jansen, ''Comparison of the effects of absorption coefficient and pulse duration of 2.12-μm and 2.79-μm radiation on laser ablation of tissue,'' *IEEE J. Quant. Elect.* **32**(12), 2025–2036 (1996).
11. E. D. Jansen, T. Assauer, M. Frenz, M. Motamedi, G. Delacretaz, and A. J. Welsh, ''Effect of pulse duration on bubble formation and laser-induced pressure waves during pulsed holmium laser ablation,'' *Lasers Surg. Med.* **18**, 278–293 (1996).
12. T. G. van Leeuwen, L. van Erven, J. H. Meertens, M. Motamedi, M. J. Post, and C. Borst, ''Origin of arterial wall dissection induced by pulsed eximer and mid-infrared laser ablation in the pig,'' *J. Am. Coll. Cardiol.* **19**, 1610–1618 (1992).
13. D. M. Davis, ''Intubated uretotomy: A new operation for ureteral ureteropelvic stricture,'' *Surg. Gyn. Obstet.* **76**, 513–516 (1943).
14. J. Schüller, H. Schuldes, G. Berendsen, and R. Nagel, ''Endoscopic intubated uretotomy,'' *Eur. Urol.* **13**, 44–48 (1987).
15. J. E. A. Wickham and M. J. Kellet, ''Percutaneous pyelolysis,'' *Eur. Urol.* **9**, 122–124 (1983).
16. R. S. Malek, ''Transurethral optical laser knife and probe director for lateral firing laser probes,'' *Proc. SPIE* **1879**, 108–111 (1993).
17. D. E. Johnson, D. M. Cromeens, and R. E. Price, ''Use of the

holmium: YAG laser in urology,'' *Lasers Surg. Med.* **12**, 353–363 (1992).
18. C. Durek, A. Knipper, R. Brinkmann, A. Miller, B. Gromoll, and D. Jocham, ''Cutting laser systems for ureteral strictures,'' *Proc. SPIE* **2086**, 112–117 (1993).
19. E. F. Maher, ''Transmission and absorption coefficients for ocular media of the rhesus monkey,'' USAF Report SAM-TR-78-32 (1979).
20. R. Brinkmann and K. Bauer, ''Q-switching and pulse shaping with IR-lasers,'' *Proc. SPIE* **1421**, 134–139 (1992).
21. O. M. Lord Rayleigh, ''On the pressure developed in a liquid during the collapse of a spherical cavity,'' *Philos. Mag. S.* **34**, 94–98 (1917).
22. J. M. Isner and R. Clarke, *Cardiovascular Laser Therapy*, pp. 39–62, Raven Press, New York (1989).
23. A. Vogel, R. Engelhardt, U. Behnle, and U. Parlitz, ''Minimization of cavitation effects in pulsed laser ablation illustrated on laser angioplasty,'' *Appl. Phys. B* **62**, 173–182 (1996).
24. R. Brinkmann, A. Knipper, G. Dröge, A. Miller, B. Gromoll, and R. Birngruber, ''Microsurgery of ureteral strictures using pulsed mid-IR lasers,'' *Proc. SPIE* **2323**, 139–146 (1994).
25. J. F. Walsh and T. F. Deutsch, ''Pulsed CO_2 laser tissue ablation: measurements of the ablation rate,'' *Lasers Surg. Med.* **8**, 264–275 (1988).
26. F. Partovi, J. A. Izatt, M. S. Feld, S. Strikwerda, and J. R. Kramer, ''Model for thermal ablation of biological tissue,'' *Proc. SPIE* **1064**, 40–44 (1989).